α-particle preformation factors in heavy and superheavy nuclei*

Song Luo (骆松)[1] Dong-Meng Zhang (张冬萌)[1] Lin-Jing Qi (亓林静)[1] Xun Chen (陈勋)[1†]
Peng-Cheng Chu (初鹏程)[2‡] Xiao-Hua Li (李小华)[1,3,4,5§]

[1]School of Nuclear Science and Technology, University of South China, Hengyang 421001, China
[2]School of Mathematics and Physics, Qingdao University of Science and Technology, Qingdao 266033, China
[3]National Exemplary Base for International Sci & Tech. Collaboration of Energy and Nuclear Safety, University of South China, Hengyang 421001, China
[4]Cooperative Innovation Center for Nuclear Fuel Cycle Technology & Equipment, University of South China, Hengyang 421001, China
[5]Key Laboratory of Low Dimensional Quantum Structures and Quantum Control, Hunan Normal University, Changsha 410081, China

Abstract: In this study, α-particle preformation factors in heavy and superheavy nuclei from ^{220}Th to ^{294}Og are investigated. By combing experimental α decay energies and half-lives, the α-particle preformation factors P_α are extracted from the ratios between theoretical α decay half-lives calculated using the Two-Potential Approach (TPA) and experimental data. We find that the α-particle preformation factors exhibit a noticeable odd-even staggering behavior, and unpaired nucleons inhibit α-particle preformation. Moreover, we find that both the α decay energy and mass number of parent nucleus exhibit considerable regularity with the extracted experimental α-particle preformation factors. After considering the major physical factors, we propose a local phenomenological formula with only five valid parameters for α-particle preformation factors P_α. This analytic expression has a clear physical meaning as well as good precision. As an application, this analytic formula is extended to estimate the α-particle preformation factors and further predict the α decay half-lives for unknown even-even nuclei with $Z = 118$ and 120.

Keywords: α decay, half-lives, preformation factors, heavy and superheavy nuclei

DOI: 10.1088/1674-1137/ad21e9

I. INTRODUCTION

α decay has long been considered a trusted pathway to obtaining nuclear structure information such as shell effects, nuclear deformation, spin and parity, and neutron-proton interaction [1−9]. This decay mode was first observed as an unknown radioactive phenomenon and further described as a process through which a parent nucleus emits a ^{4}He particle by Rutherford [10]. Until the 1920s, the corresponding decay mechanism was explained as a quantum tunneling effect by Gamow [11] and Condon and Gurney [12]. Since then, numerous models and/or phenomenological formulae based on tunneling theory have been proposed to calculate α decay half-lives and further reconstruct the corresponding decay process [13−21].

Generally, the numerous approaches on α decay can be divided into two categories: the cluster-like and fission-like theories. The main difference between these two theories lies in the treatment of whether the α-particle is preformed in the parent nucleus [22]. Consequently, the corresponding decay constant frequently has different forms. In the fission-like theory, the decay constant λ can be defined as the product of two terms: the penetration probability and effective assault frequency. Note that the effective assault frequency contains the certain α-particle preformation information [23, 24]. Correspondingly, the decay constant λ in the preformed cluster models can be described as the product of three physical terms: the α-particle preformation factor, penetration probability, and collision probability. Among these three terms, the α-particle preformation factor is an indispensable physical concept; it represents the relative probability that the α-particle exists as an entity on the surface of or inside the parent nucleus. In practice, it is largely dependent on the

Received 27 October 2023; Accepted 24 January 2024; Published online 25 January 2024

* Supported in part by the National Natural Science Foundation of China (12175100, 11975132), the Construct Program of the Key Discipline in Hunan Province, the Research Foundation of Education Bureau of Hunan Province, China (21B0402, 18A237, 22A0305), the Natural Science Foundation of Hunan Province, China (2018JJ2321), the Innovation Group of Nuclear and Particle Physics in USC, the Shandong Province Natural Science Foundation, China (ZR2022JQ04) and the Opening Project of Cooperative Innovation Center for Nuclear Fuel Cycle Technology and Equipment, University of South China (2019KFZ10), Hunan Provincial Innovation Foundation for Postgraduate (CX20230962)

† E-mail: chenxunhep@qq.com
‡ E-mail: kyois@126.com
§ E-mail: lixiaohuaphysics@126.com

©2024 Chinese Physical Society and the Institute of High Energy Physics of the Chinese Academy of Sciences and the Institute of Modern Physics of the Chinese Academy of Sciences and IOP Publishing Ltd

structure and state of parent and daughter nuclei. Therefore, the preformation factor has an essential role in the exploration of nuclear structure [25]. However, reasonably evaluating the α-particle preformation factor is challenging as it is not a valid observation quantity. Several methods have been proposed to evaluate or extract α-particle preformation factors, such as the R-matrix method [26−28], microscopic wave function approach [29, 30], cluster-formation model [31−33], density-dependent cluster model [34], generalized liquid drop model [35−38], and Two-Potential Approach (TPA) [39−41]. In general, the above mentioned methods obtain the preformation factors through the ratios between theoretical α decay half-lives and experimental data. In these cases, most of the obtained preformation factors are model dependent because the matched integration form differs for various models.

The TPA is one of the excellent phenomenological models used to investigate the α decay process. Currently, α-particle preformation factors P_α are poorly studied in the TPA framework, particularly for heavy and superheavy nuclei. On the one hand, exploring the hidden nuclear structure information can provide valuable reference for further exploration. On the other hand, this model must be urgently refined to provide more reliable predictions for future experiments. Hence, we systemically study the preformation factors in the heavy and superheavy region from ^{220}Th to ^{294}Og. Referring to relevant studies [42, 43], this work primarily focuses on the ground-state α transitions. Subsequently, we discuss the corresponding nuclear structure information in detail. We propose a local phenomenological formula with only five valid parameters for α-particle preformation factors P_α. This analytical expression can be used to evaluate the α-particle preformation factors and accurately calculate half-lives. With this analytic formula, we predict the α decay half-lives for unknown even-even nuclei with Z = 118 and 120.

The remainder of this article is organized as follows. In Sec. II, the theoretical framework of the TPA is briefly described. The detailed results and discussion are presented in Sec. III. Finally, a succinct summary is provided in Sec. IV.

II. THEORETICAL FRAMEWORK

A. TPA framework

In the TPA, the α decay half-lives $T_{1/2}$ can be defined as

$$T_{1/2} = \frac{\ln 2}{\lambda} = \frac{\hbar \ln 2}{\Gamma}, \tag{1}$$

where λ and Γ represent the decay constant and decay width, respectively. In general, the decay constant and decay width are related to three parts, which are the normalized factor F, penetration probability P, and α-particle preformation factor P_α. Within the TPA framework, the decay width can be expressed as

$$\Gamma = \frac{\hbar^2 F P P_\alpha}{4\mu}. \tag{2}$$

F is an important physical quantity related to the collision probability or assault frequency, which satisfies the condition

$$F\int_{r_1}^{r_2} \frac{1}{2k(r)}\mathrm{d}r = 1, \tag{3}$$

where r is the mass center distance between daughter nucleus and preformed α-particle. Note that F appears as the normalized factor of the bound state wave function, which is essential in describing the frequency of particle motion in the quasi-classical period. Moreover, the condition in Eq. (3) is a key constraint for the bound state wave function. Details of the integral form are available in Ref. [44]. $k(r)$ represents the wave number, which can be given by

$$k(r) = \sqrt{\frac{2\mu}{\hbar^2}|Q_\alpha - V(r)|}, \tag{4}$$

where $V(r)$ and Q_α denote total interaction potential and α decay energy, respectively. μ is the reduced mass of the α-particle and daughter nucleus and can be described as $\mu = \frac{m_\alpha m_d}{m_\alpha + m_d}$, where m_α and m_d represent the nucleon mass of the α-particle and daughter nucleus, respectively. The penetration probability P represents the probability that α-particle penetrates the barrier. It can be given by

$$P = \exp\left[-2\int_{r_2}^{r_3} k(r)\mathrm{d}r\right], \tag{5}$$

where r_1, r_2, and r_3 are the classical turning points and satisfy the conditions $V(r_1) = V(r_2) = V(r_3) = Q_\alpha$. In the parent nucleus ($r_1 < r < r_2$), the corresponding interactions are dominated by the nuclear potential, whereas, in the region outside the nucleus ($r_2 < r < r_3$), the Coulomb potential has an important role.

The total interaction potential includes three parts: the nuclear potential $V_N(r)$, Coulomb potential $V_C(r)$, and centrifugal potential $V_l(r)$. It can be expressed as

$$V(r) = V_N(r) + V_C(r) + V_l(r). \tag{6}$$

In this work, the nuclear potential is described by the type of cosh parametrized form, which can be expressed as

$$V_N(r) = -V_0 \frac{1+\cosh(R/a)}{\cosh(r/a)+\cosh(R/a)}, \tag{7}$$

where V_0 and a are parameters of the depth and diffuseness of the nuclear potential, respectively. In our previous study [39], a series of parameter values were obtained with $a = 0.5958$ fm and $V_0 = 192.42 + 31.059\frac{N-Z}{A}$ MeV, where N, Z, and A are the neutron, proton, and mass number of daughter nucleus, respectively. $V_C(r)$ represents the Coulomb potential, which is based on the assumption of the uniformly charged sphere and can be described as

$$V_C(r) = \begin{cases} \dfrac{Z_d Z_\alpha e^2}{2R}\left[3 - \dfrac{r^2}{R^2}\right], & r \le R, \\ \dfrac{Z_d Z_\alpha e^2}{r}, & r > R, \end{cases} \tag{8}$$

where Z_d and Z_α are the charge number of the daughter nucleus and α-particle, respectively. The radius R is given by

$$R = 1.28A^{1/3} - 0.76 + 0.8A^{-1/3}. \tag{9}$$

For unfavored α decay ($\ell \neq 0$ decays, where ℓ represents the angular momentum obtained by the emitted α-particle), the corresponding centrifugal potential generated by the nonzero angular momentum can be considered as

$$V_l(r) = \frac{\hbar^2(l+\frac{1}{2})^2}{2\mu r^2}. \tag{10}$$

Eq. (10) is related to the Langer modified form because the term $l(l+1) \rightarrow (l+1/2)^2$ is an important correction for one-dimensional problems [45]. The minimum angular momentum $\ell_{\min}$ obtained by the α-particle is selected in based on the conservation laws of spin-parity, which is given by

$$\ell_{\min} = \begin{cases} \Delta_j, & \text{for even } \Delta_j \text{ and } \pi_p = \pi_d, \\ \Delta_j + 1, & \text{for even } \Delta_j \text{ and } \pi_p \neq \pi_d, \\ \Delta_j, & \text{for odd } \Delta_j \text{ and } \pi_p = \pi_d, \\ \Delta_j + 1, & \text{for odd } \Delta_j \text{ and } \pi_p \neq \pi_d, \end{cases} \tag{11}$$

where $\Delta_j = |j_p - j_d|$, j_p, π_p, j_d, π_d represent the spin and parity values of parent and daughter nuclei, respectively. Details on the conservation laws of spin-parity are available in the Ref. [46].

B. α-particle preformation factors P_α

Referring to Eqs. (1) and (2), the experimental decay constant $\lambda_{\rm exp}$ can be calculated as

$$\lambda_{\rm exp} = \frac{\ln 2}{T_{1/2}^{\rm exp}} = \frac{\hbar P_\alpha^{\rm exp} FP}{4\mu}. \tag{12}$$

Correspondingly, if the α-particle preformation factor is fixed as $P_0 = 1$, the theoretical decay constant $\lambda_{\rm cal}$ can be given by

$$\lambda_{\rm cal} = \frac{\ln 2}{T_{1/2}^{\rm cal}} = \frac{\hbar P_0 FP}{4\mu}. \tag{13}$$

Combining the Eqs. (12) and (13), the α-particle preformation factors can be extracted from the ratios between theoretical α decay half-lives and experimental data. It can be expressed as

$$P_\alpha^{\rm exp} = \frac{\lambda_{\rm exp}}{\lambda_{\rm cal}} = \frac{T_{1/2}^{\rm cal}}{T_{1/2}^{\rm exp}}. \tag{14}$$

Note that α-particle preformation factors extracted using Eq. (14) are not the absolute values; they reflect only the relative probabilities of the α-particle forming inside or on the surface of the parent nucleus.

III. RESULTS AND DISCUSSION

The TPA is widely used to study the α decay process [39, 47, 48] and proton radioactivity [49], and the corresponding results agree closely with experimental data. In this work, the α-particle preformation factors P_α for heavy and superheavy nuclei are extracted from the ratios between theoretical α decay half-lives calculated using the TPA and experimental data. The detailed results for 65 even-even, 87 odd-A, and 28 odd-odd nuclei are listed in Tables 1−3, respectively. These three tables share the same framework; the first five columns denote the α transition, corresponding decay energies (Q_α), spin and parity for parent and daughter nuclei, and minimum angular momentum taken away by the emitted α-particle, respectively. The middle five columns represent the logarithmic value of experimental α decay half-lives, normalized factor F, penetration probability P, and experimental α-particle preformation factors extracted from Eq. (14), denoted as $P_\alpha^{\rm exp}$, and those estimated using Eq. (15), denoted as $P_\alpha^{\rm Eq}$, respectively. The last two columns denote the calculated α decay half-lives in logarithmic form with the corresponding preformation factors derived from the fixed $P_0 = 1.0$ and Eq. (15), denoted as $\log_{10}T_{1/2}^{\rm cal1}$ and

Table 1. Calculations of α-particle preformation factors and α decay half-lives for 65 even-even nuclei. The experimental α decay half-lives, spin, and parity are obtained from Refs. [46, 50, 51]. The α decay energy values are obtained from the latest evaluated atomic mass table AME2020 [52, 53]. The decay energy and half-lives are in the units of MeV and s, respectively.

α transition	Q_α	j_p^π	j_d^π	$\ell_{\min}$	$\log_{10}T_{1/2}^{\exp}$	F	P	$P_\alpha^{\exp}$	P_α^{Eq}	$\log_{10}T_{1/2}^{\mathrm{cal1}}$	$\log_{10}T_{1/2}^{\mathrm{cal2}}$
^{220}Th→^{216}Ra	8.97	0^+	0^+	0	−5.01	0.859	3.455×10^{-17}	0.5902	0.4399	−5.24	−4.88
^{222}Th→^{218}Ra	8.13	0^+	0^+	0	−2.69	0.861	1.595×10^{-19}	0.6108	0.4692	−2.90	−2.58
^{224}Th→^{220}Ra	7.30	0^+	0^+	0	0.12	0.861	3.007×10^{-22}	0.5017	0.5102	−0.18	0.11
^{226}Th→^{222}Ra	6.45	0^+	0^+	0	3.39	0.876	1.324×10^{-25}	0.6021	0.5723	3.17	3.41
^{228}Th→^{224}Ra	5.52	0^+	0^+	0	7.93	0.805	3.482×10^{-30}	0.7179	0.6823	7.79	7.95
^{230}Th→^{226}Ra	4.77	0^+	0^+	0	12.49	0.874	7.533×10^{-35}	0.8421	0.8158	12.42	12.50
^{232}Th→^{228}Ra	4.08	0^+	0^+	0	17.76	0.825	2.867×10^{-40}	1.2594	1.0123	17.86	17.85
^{222}U→^{218}Th	9.48	0^+	0^+	0	−5.33	0.848	1.373×10^{-16}	0.3146	0.4090	−5.83	−5.44
^{224}U→^{220}Th	8.63	0^+	0^+	0	−3.39	0.824	8.512×10^{-19}	0.5992	0.4336	−3.61	−3.25
^{226}U→^{222}Th	7.70	0^+	0^+	0	−0.57	0.869	1.169×10^{-21}	0.6269	0.4751	−0.77	−0.45
^{228}U→^{224}Th	6.80	0^+	0^+	0	2.90	0.874	5.231×10^{-25}	0.4720	0.5332	2.57	2.85
^{230}U→^{226}Th	5.99	0^+	0^+	0	6.43	0.856	1.115×10^{-28}	0.6669	0.6076	6.25	6.47
^{232}U→^{228}Th	5.41	0^+	0^+	0	9.50	0.867	8.207×10^{-32}	0.7615	0.6733	9.38	9.55
^{234}U→^{230}Th	4.86	0^+	0^+	0	13.04	0.883	2.621×10^{-35}	0.6755	0.7595	12.87	12.99
^{236}U→^{232}Th	4.57	0^+	0^+	0	15.00	0.876	2.174×10^{-37}	0.9005	0.7982	14.95	15.05
^{238}U→^{234}Th	4.27	0^+	0^+	0	17.25	0.755	8.980×10^{-40}	1.4219	0.8515	17.40	17.47
^{230}Pu→^{226}U	7.18	0^+	0^+	0	2.01	0.875	2.401×10^{-24}	0.7971	0.4951	1.91	2.22
^{232}Pu→^{228}U	6.72	0^+	0^+	0	4.13	0.873	3.399×10^{-26}	0.4279	0.5148	3.76	4.05
^{234}Pu→^{230}U	6.31	0^+	0^+	0	5.89	0.876	5.122×10^{-28}	0.4920	0.5344	5.58	5.85
^{236}Pu→^{232}U	5.87	0^+	0^+	0	8.11	0.873	3.382×10^{-30}	0.4506	0.5649	7.76	8.01
^{238}Pu→^{234}U	5.59	0^+	0^+	0	9.59	0.876	1.044×10^{-31}	0.4822	0.5774	9.27	9.51
^{240}Pu→^{236}U	5.26	0^+	0^+	0	11.45	0.877	1.170×10^{-33}	0.5929	0.6035	11.22	11.44
^{242}Pu→^{238}U	4.98	0^+	0^+	0	13.18	0.887	1.830×10^{-35}	0.6979	0.6262	13.02	13.23
^{244}Pu→^{240}U	4.67	0^+	0^+	0	15.50	0.875	1.155×10^{-37}	0.5366	0.6627	15.23	15.41
^{234}Cm→^{230}Pu	7.37	0^+	0^+	0	2.11	0.825	2.057×10^{-24}	0.7923	0.4519	2.00	2.35
^{236}Cm→^{232}Pu	7.07	0^+	0^+	0	3.35	0.873	1.472×10^{-25}	0.5958	0.4536	3.13	3.47
^{238}Cm→^{234}Pu	6.67	0^+	0^+	0	5.51	0.846	3.143×10^{-27}	0.1992	0.4677	4.81	5.14
^{240}Cm→^{236}Pu	6.40	0^+	0^+	0	6.52	0.826	1.953×10^{-28}	0.3210	0.4711	6.03	6.35
^{242}Cm→^{238}Pu	6.22	0^+	0^+	0	7.28	0.879	2.846×10^{-29}	0.3599	0.4658	6.84	7.17
^{244}Cm→^{240}Pu	5.90	0^+	0^+	0	8.87	0.820	6.784×10^{-31}	0.4159	0.4793	8.49	8.81
^{246}Cm→^{242}Pu	5.48	0^+	0^+	0	11.26	0.874	2.905×10^{-33}	0.3711	0.5119	10.83	11.12
^{248}Cm→^{244}Pu	5.16	0^+	0^+	0	13.16	0.835	2.943×10^{-35}	0.4832	0.5368	12.84	13.11
^{238}Cf→^{234}Cm	8.13	0^+	0^+	0	−0.08	0.806	1.889×10^{-22}	1.3545	0.3722	0.05	0.48
^{240}Cf→^{236}Cm	7.71	0^+	0^+	0	2.03	0.866	7.027×10^{-24}	0.2629	0.3795	1.45	1.87
^{242}Cf→^{238}Cm	7.52	0^+	0^+	0	2.54	0.867	1.520×10^{-24}	0.3755	0.3720	2.11	2.54
^{244}Cf→^{240}Cm	7.33	0^+	0^+	0	3.06	0.812	3.078×10^{-25}	0.5978	0.3654	2.84	3.27
^{246}Cf→^{242}Cm	6.86	0^+	0^+	0	5.11	0.830	3.741×10^{-27}	0.4288	0.3820	4.74	5.16
^{248}Cf→^{244}Cm	6.36	0^+	0^+	0	7.56	0.827	1.947×10^{-27}	0.2936	0.4067	7.03	7.42
^{250}Cf→^{246}Cm	6.13	0^+	0^+	0	8.69	0.860	1.460×10^{-30}	0.2790	0.4085	8.14	8.52
^{252}Cf→^{248}Cm	6.22	0^+	0^+	0	8.01	0.834	4.700×10^{-30}	0.4276	0.3780	7.64	8.06

Continued on next page

Table 1-continued from previous page

α transition	Q_α	j_p^π	j_d^π	$\ell_{\min}$	$\log_{10}T_{1/2}^{\exp}$	F	P	$P_\alpha^{\exp}$	P_α^{Eq}	$\log_{10}T_{1/2}^{\mathrm{cal1}}$	$\log_{10}T_{1/2}^{\mathrm{cal2}}$
^{254}Cf→^{250}Cm	5.93	0^+	0^+	0	9.31	0.866	1.505×10^{-31}	0.6448	0.3869	9.12	9.53
^{244}Fm→^{240}Cf	8.55	0^+	0^+	0	−0.51	0.850	9.260×10^{-22}	0.7051	0.3105	−0.66	−0.15
^{246}Fm→^{242}Cf	8.38	0^+	0^+	0	0.17	0.842	2.892×10^{-22}	0.4765	0.3023	−0.15	0.37
^{248}Fm→^{244}Cf	7.99	0^+	0^+	0	1.66	0.832	1.504×10^{-23}	0.3002	0.3063	1.14	1.65
^{250}Fm→^{246}Cf	7.56	0^+	0^+	0	3.38	0.792	4.302×10^{-25}	0.2100	0.3144	2.70	3.20
^{252}Fm→^{248}Cf	7.15	0^+	0^+	0	5.04	0.812	1.063×10^{-26}	0.1814	0.3238	4.30	4.79
^{254}Fm→^{250}Cf	7.31	0^+	0^+	0	4.14	0.790	5.371×10^{-26}	0.2929	0.2967	3.61	4.13
^{256}Fm→^{252}Cf	7.03	0^+	0^+	0	5.14	0.838	3.985×10^{-27}	0.3724	0.2984	4.71	5.24
^{252}No→^{248}Fm	8.55	0^+	0^+	0	0.74	0.845	2.179×10^{-22}	0.1696	0.2638	−0.03	0.55
^{254}No→^{250}Fm	8.23	0^+	0^+	0	1.82	0.848	2.047×10^{-23}	0.1496	0.2640	0.99	1.57
^{256}No→^{252}Fm	8.58	0^+	0^+	0	0.53	0.828	3.309×10^{-22}	0.1848	0.2357	−0.20	0.42
^{256}Rf→^{252}No	8.93	0^+	0^+	0	0.32	0.869	6.876×10^{-22}	0.1375	0.2353	−0.54	0.09
^{258}Rf→^{254}No	9.20	0^+	0^+	0	−0.61	0.853	4.952×10^{-21}	0.1656	0.2139	−1.39	−0.72
^{260}Sg→^{256}Rf	9.90	0^+	0^+	0	−2.04	0.860	9.918×10^{-20}	0.2379	0.1932	−2.66	−1.95
^{266}Hs→^{262}Sg	10.35	0^+	0^+	0	−2.41	0.852	3.574×10^{-19}	0.1450	0.1634	−3.25	−2.46
^{268}Hs→^{264}Sg	9.77	0^+	0^+	0	−0.39	0.836	1.116×10^{-20}	0.0452	0.1680	−1.73	-0.96
^{270}Hs→^{266}Sg	9.07	0^+	0^+	0	1.18	0.826	1.035×10^{-22}	0.1327	0.1775	0.30	1.05
^{270}Ds→^{266}Hs	11.12	0^+	0^+	0	−2.70	0.841	6.663×10^{-18}	0.0154	0.1404	−4.51	−3.66
^{282}Ds→^{278}Hs	9.15	0^+	0^+	0	1.82	0.837	5.506×10^{-23}	0.0565	0.1363	0.57	1.44
^{286}Cn→^{282}Ds	9.24	0^+	0^+	0	1.48	0.820	2.180×10^{-23}	0.3208	0.1282	0.98	1.88
^{286}Fl→^{282}Cn	10.36	0^+	0^+	0	−0.66	0.845	7.558×10^{-21}	0.1231	0.1141	−1.57	−0.63
^{288}Fl→^{284}Cn	10.08	0^+	0^+	0	−0.19	0.758	1.401×10^{-21}	0.2507	0.1130	−0.79	0.16
^{290}Lv→^{286}Fl	11.00	0^+	0^+	0	−2.05	0.838	8.488×10^{-20}	0.2712	0.0997	−2.62	−1.62
^{292}Lv→^{288}Fl	10.79	0^+	0^+	0	−1.80	0.839	2.728×10^{-20}	0.4743	0.0976	−2.12	−1.11
^{294}Og→^{290}Lv	11.87	0^+	0^+	0	−3.15	0.769	2.592×10^{-18}	0.1219	0.0855	−4.06	−3.00

$\log_{10}T_{1/2}^{\mathrm{cal2}}$, respectively.

Table 1 shows that the normalized factor F always remains within a small range, and the experimental half-lives increases with the neutron number N in each isotope chain. The increased neutrons may contribute significantly to maintaining the nuclear stability. Wang *et al.* suggest the increasing symmetry energy leads to this behavior [54]. In contrast, the decay energy Q_α and penetration probability P decrease gradually in each isotope chain. The penetration probabilities for different nuclei have very large discrepancies with a given isotope chain, indicating that the penetration probability largely determines the α decay half-lives. More importantly, as shown in the ninth column, the penetration probability is always within a narrow range of 10^{-22} and 10^{-18} for the $Rf-Og$ (Z = 104 - 118) isotope chain. The relatively large penetration probability means that the α-particle can easily escape from the parent nuclei and the superheavy nuclei should be weakly bound [55].

For preformation factors, by combining the three tables, we find that the sequence of nuclei in the order of decreasing $P_\alpha^{\exp}$ is even-even, odd-A, and odd-odd nuclei. The results satisfy the variation trend of α-particle preformation factors extracted using various models [56−58]. For a more intuitive description, the extracted experimental α-particle preformation factors for Th and Pa isotopes are plotted as black squares and red balls, respectively, in Fig. 1. This figure shows that the preformation factors of even-even nuclei are significantly larger than the corresponding ones of the adjacent odd-A nuclei from Th isotopes. Additionally, the corresponding preformation factors of odd-A nuclei are larger than the corresponding ones of the adjacent odd-odd nuclei in the Pa isotopes. This result suggests that the unpaired nucleons will inhibit α-particle preformation. Note that these regularities are analyzed through the overall performance. Strictly, the preformation factors are strongly correlated with the nuclear structure. Zhang *et al.* proved that the nuclei near the closed shell are relatively stable owing to the strong bound states [55]. Thus, the preforming factors

Table 2. Same as Table 1 but for 87 odd-A nuclei. "*," "#," and "()" indicate values estimated from trends in neighboring nuclei, uncertain spin, and uncertain parity, respectively.

α transition	Q_α	J_p^π	J_d^π	$\ell_{\min}$	$\log_{10}T_{1/2}^{\exp}$	F	P	$P_\alpha^{\exp}$	P_α^{Eq}	$\log_{10}T_{1/2}^{\mathrm{cal1}}$	$\log_{10}T_{1/2}^{\mathrm{cal2}}$
^{221}Th→^{217}Ra	8.63	$7/2^+$#	$(9/2^+)$	2	−2.76	0.873	2.532×10^{-18}	0.0446	0.1123	−4.11	−3.16
^{223}Th→^{219}Ra	7.57	$(5/2)^+$	$(7/2)^+$	2	−0.22	0.876	1.465×10^{-21}	0.2216	0.1254	−0.87	0.03
^{225}Th→^{221}Ra	6.92	$3/2^+$	$5/2^+$*	2	2.77	0.866	6.527×10^{-24}	0.0515	0.1336	1.48	2.36
^{227}Th→^{223}Ra	6.15	$(1/2^+)$	$3/2^+$*	2	6.21	0.875	3.325×10^{-27}	0.0363	0.1494	4.77	5.60
^{229}Th→^{225}Ra	5.17	$5/2^+$*	$1/2^+$	2	11.39	0.863	1.752×10^{-32}	0.0462	0.1843	10.05	10.79
^{221}Pa→^{217}Ac	9.24	$9/2^-$	$9/2^-$	0	−5.23	0.838	7.637×10^{-17}	0.4534	0.1438	−5.57	−4.73
^{223}Pa→^{219}Ac	8.35	$9/2^-$	$9/2^-$	0	−2.15	0.860	3.065×10^{-19}	0.0918	0.1539	−3.19	−2.37
^{225}Pa→^{221}Ac	7.41	$5/2^-$#	$9/2^-$#	2	0.23	0.872	1.647×10^{-22}	0.7018	0.1254	0.08	0.98
^{227}Pa→^{223}Ac	6.58	$(5/2^-)$	$(5/2^-)$	0	3.43	0.872	1.712×10^{-25}	0.4260	0.1895	3.06	3.78
^{229}Pa→^{225}Ac	5.84	$5/2^+$	$3/2^-$	1	7.40	0.882	4.832×10^{-29}	0.1601	0.1792	6.60	7.35
^{231}Pa→^{227}Ac	5.15	$3/2^-$*	$3/2^-$*	0	12.00	0.869	7.156×10^{-33}	0.0276	0.2462	10.44	11.05
^{223}U→^{219}Th	9.17	$7/2^+$#	$9/2^+$#	2	−4.74	0.791	1.392×10^{-17}	0.8552	0.1037	−4.81	−3.82
^{225}U→^{221}Th	8.01	$5/2^+$	$7/2^+$#	2	−1.16	0.869	6.834×10^{-21}	0.4170	0.1163	−1.54	−0.61
^{227}U→^{223}Th	7.24	$(3/2^+)$	$(5/2^+)$	2	1.82	0.868	1.569×10^{-23}	0.1904	0.1259	1.10	2.00
^{229}U→^{225}Th	6.48	$3/2^+$	$3/2^+$	0	4.24	0.823	2.288×10^{-26}	0.5238	0.1888	3.96	4.68
^{231}U→^{227}Th	5.58	$5/2^+$#	$(1/2^+)$	2	9.82	0.828	4.231×10^{-31}	0.0740	0.1652	8.69	9.47
^{233}U→^{229}Th	4.91	$5/2^+$*	$5/2^+$*	0	12.69	0.891	5.536×10^{-35}	0.7096	0.2610	12.54	13.12
^{223}Np→^{219}Pa	9.66	$(9/2^-)$	$9/2^-$	0	−5.66	0.858	1.728×10^{-16}	0.5281	0.1355	−5.94	−5.05
^{225}Np→^{221}Pa	8.83	$9/2^-$#	$9/2^-$	0	−2.44	0.851	1.347×10^{-18}	0.0412	0.1429	−3.83	−2.98
^{227}Np→^{223}Pa	7.82	$5/2^+$#	$9/2^-$#	3	−0.29	0.873	3.964×10^{-22}	0.9648	0.1028	−0.31	0.68
^{229}Np→^{225}Pa	7.02	$5/2^+$	$5/2^-$#	1	2.55	0.702	1.250×10^{-24}	0.5501	0.1455	2.29	3.13
^{231}Np→^{227}Pa	6.37	$5/2^+$#	$(5/2^-)$	1	5.16	0.839	2.161×10^{-27}	0.6539	0.1584	4.98	5.78
^{233}Np→^{229}Pa	5.63	$5/2^+$#	$5/2^+$	0	8.49	0.847	4.674×10^{-31}	1.4010	0.2160	8.64	9.30
^{235}Np→^{231}Pa	5.19	$5/2^+$	$3/2^-$*	1	12.12	0.861	9.755×10^{-34}	0.1548	0.1954	11.31	12.02
^{237}Np→^{233}Pa	4.96	$5/2^+$*	$3/2^-$	1	13.83	0.854	3.241×10^{-35}	0.0917	0.1993	12.79	13.49
^{229}Pu→^{225}U	7.59	$3/2^+$#	$5/2^+$	2	1.95	0.858	4.507×10^{-23}	0.0497	0.1181	0.65	1.57
^{231}Pu→^{227}U	6.84	$(3/2^+)$	$(3/2^+)$	0	3.71	0.860	1.053×10^{-25}	0.3692	0.1754	3.28	4.03
^{233}Pu→^{229}U	6.41	$5/2^+$#	$3/2^+$	2	6.00	0.853	8.244×10^{-28}	0.2436	0.1346	5.39	6.26
^{235}Pu→^{231}U	5.95	$(5/2^+)$	$5/2^+$#	0	7.73	0.852	8.520×10^{-30}	0.4395	0.1934	7.37	8.09
^{241}Pu→^{237}U	5.14	$5/2^+$*	$1/2^+$	2	13.26	0.847	1.172×10^{-34}	0.0949	0.1529	12.24	13.05
^{229}Am→^{225}Np	8.14	$5/2^-$#	$9/2^-$#	2	−0.01	0.867	1.294×10^{-21}	0.1563	0.1104	−0.82	0.14
^{233}Am→^{229}Np	7.07	$5/2^-$#	$5/2^+$	1	3.63	0.884	3.000×10^{-25}	0.1515	0.1366	2.81	3.67
^{235}Am→^{231}Np	6.58	$5/2^-$#	$5/2^+$#	1	5.19	0.862	2.642×10^{-27}	0.4863	0.1435	4.88	5.72
^{237}Am→^{233}Np	6.20	$5/2^-$	$5/2^+$#	1	7.24	0.853	4.601×10^{-29}	0.2512	0.1486	6.64	7.47
^{239}Am→^{235}Np	5.92	$5/2^-$	$5/2^+$	1	8.63	0.840	1.840×10^{-30}	0.2600	0.1510	8.04	8.87
^{241}Am→^{237}Np	5.64	$5/2^-$*	$5/2^+$*	1	10.13	0.861	5.715×10^{-32}	0.2583	0.1544	9.54	10.35
^{243}Am→^{239}Np	5.44	$5/2^-$*	$5/2^+$	1	11.37	0.870	4.146×10^{-33}	0.2027	0.1550	10.68	11.49
^{233}Cm→^{229}Pu	7.48	$3/2^+$#	$3/2^+$#	0	2.06	0.807	5.111×10^{-24}	0.3619	0.1547	1.62	2.43
^{235}Cm→^{231}Pu	7.28	$5/2^+$#	$(3/2^+)$	2	4.47	0.872	5.613×10^{-25}	0.0119	0.1120	2.54	3.49
^{241}Cm→^{237}Pu	6.19	$1/2^+$	$7/2^-$	3	8.45	0.867	6.323×10^{-30}	0.1110	0.1066	7.50	8.47

Continued on next page

Table 2-continued from previous page

α transition	Q_α	j_p^π	j_d^π	$\ell_{\min}$	$\log_{10}T_{1/2}^{\exp}$	F	P	$P_\alpha^{\exp}$	P_α^{Eq}	$\log_{10}T_{1/2}^{\mathrm{cal1}}$	$\log_{10}T_{1/2}^{\mathrm{cal2}}$
^{243}Cm→^{239}Pu	6.17	$5/2^+*$	$1/2^+*$	2	8.96	0.822	9.640×10^{-30}	0.0237	0.1150	7.34	8.27
^{245}Cm→^{241}Pu	5.62	$7/2^+*$	$5/2^+*$	2	11.42	0.867	1.081×10^{-32}	0.0696	0.1265	10.26	11.16
^{247}Cm→^{243}Pu	5.35	$9/2^-*$	$7/2^+$	1	14.69	0.861	3.967×10^{-34}	0.0010	0.1478	11.70	12.53
^{245}Bk→^{241}Am	6.45	$3/2^-$	$5/2^-*$	2	8.55	0.843	8.184×10^{-29}	0.0070	0.1049	6.40	7.37
^{247}Bk→^{243}Am	5.89	$3/2^-$	$5/2^-*$	2	10.64	0.858	1.214×10^{-31}	0.0377	0.1147	9.22	10.16
^{249}Bk→^{245}Am	5.52	$7/2^+*$	$5/2^+$	2	12.32	0.827	9.715×10^{-34}	0.1022	0.1209	11.33	12.25
^{237}Cf→^{233}Cm	8.23	$5/2^+$#	$3/2^+$#	2	0.06	0.864	2.272×10^{-22}	0.7605	0.0943	−0.06	0.97
^{239}Cf→^{235}Cm	7.77	$5/2^+$#	$5/2^+$#	0	1.63	0.794	1.104×10^{-23}	0.4588	0.1312	1.27	2.17
^{243}Cf→^{239}Cm	7.42	$(1/2^+)$	$7/2^-$#	3	3.66	0.801	2.258×10^{-25}	0.2075	0.0815	2.98	4.07
^{245}Cf→^{241}Cm	7.26	$1/2^+$	$1/2^+$	0	3.89	0.866	1.701×10^{-25}	0.1500	0.1225	3.07	3.98
^{247}Cf→^{243}Cm	6.50	$(7/2^+)$	$5/2^+*$	2	7.50	0.904	5.137×10^{-29}	0.1168	0.1012	6.57	7.56
^{249}Cf→^{245}Cm	6.29	$9/2^-$	$7/2^+*$	1	10.04	0.876	7.643×10^{-30}	0.0023	0.1148	7.41	8.35
^{251}Cf→^{247}Cm	6.18	$1/2^+$	$9/2^-*$	5	10.45	0.866	1.853×10^{-31}	0.0379	0.0675	9.03	10.20
^{243}Es→^{239}Bk	8.08	$(7/2^+)$	$(7/2^+)$	0	1.55	0.783	6.317×10^{-23}	0.0977	0.1142	0.54	1.48
^{249}Es→^{245}Bk	6.94	$7/2^+$	$3/2^-$	3	6.03	0.840	1.139×10^{-27}	0.1673	0.0788	5.25	6.36
^{251}Es→^{247}Bk	6.60	$3/2^-$	$3/2^-$	0	7.37	0.832	1.059×10^{-28}	0.0830	0.1241	6.29	7.20
^{253}Es→^{249}Bk	6.74	$7/2^+*$	$7/2^+*$	0	6.25	0.853	5.207×10^{-28}	0.2173	0.1137	5.59	6.53
^{243}Fm→^{239}Cf	8.70	$7/2^-$#	$5/2^+$#	1	−0.60	0.838	2.185×10^{-21}	0.3729	0.0888	−1.03	0.02
^{245}Fm→^{241}Cf	8.44	$1/2^+$#	$7/2^-$#	3	0.62	0.864	1.522×10^{-22}	0.3128	0.0680	0.12	1.28
^{247}Fm→^{243}Cf	8.26	$(7/2^+)$	$(1/2^+)$	4	1.68	0.869	2.141×10^{-23}	0.1927	0.0585	0.96	2.20
^{251}Fm→^{247}Cf	7.43	$9/2^-$	$(7/2^+)$	1	6.02	0.867	1.177×10^{-25}	0.0016	0.0895	3.23	4.27
^{257}Fm→^{253}Cf	6.86	$9/2^+$	$7/2^+$	2	6.94	0.816	4.393×10^{-28}	0.0550	0.0756	5.68	6.80
^{245}Md→^{241}Es	9.02	$(7/2^-)$	$3/2^-$#	2	−0.48	0.857	6.472×10^{-21}	0.0935	0.0723	−1.51	−0.37
^{247}Md→^{243}Es	8.77	$7/2^-$#	$(7/2^+)$	1	0.08	0.853	1.774×10^{-21}	0.0944	0.0809	−0.95	0.15
^{249}Md→^{245}Es	8.44	$(7/2^-)$	$(3/2^-)$	2	1.54	0.855	1.237×10^{-22}	0.0468	0.0711	0.21	1.36
^{251}Md→^{247}Es	7.96	$(7/2^-)$	$(7/2^+)$	1	3.40	0.869	4.349×10^{-24}	0.0181	0.0833	1.66	2.74
^{253}Md→^{249}Es	7.57	$(7/2^-)$	$7/2^+$	1	4.71	0.850	1.673×10^{-25}	0.0235	0.0849	3.08	4.15
^{255}Md→^{251}Es	7.91	$(7/2^-)$	$3/2^-$	2	4.36	0.827	2.468×10^{-24}	0.0037	0.0663	1.92	3.10
^{257}Md→^{253}Es	7.56	$(7/2^-)$	$7/2^+*$	1	5.12	0.866	1.861×10^{-25}	0.0081	0.0765	3.03	4.14
^{251}No→^{247}Fm	8.76	$(7/2^+)$	$(7/2^+)$	0	−0.02	0.836	9.666×10^{-22}	0.2225	0.0890	−0.67	0.38
^{253}No→^{249}Fm	8.42	$9/2^-*$	$7/2^+$	1	2.23	0.781	7.212×10^{-23}	0.0179	0.0748	0.48	1.61
^{257}No→^{253}Fm	8.48	$(3/2^+)$	$1/2^+$	2	1.46	0.870	9.831×10^{-23}	0.0696	0.0585	0.30	1.54
^{259}No→^{255}Fm	7.85	$9/2^+$	$7/2^+$	2	3.66	0.863	6.814×10^{-25}	0.0638	0.0620	2.47	3.67
^{253}Lr→^{249}Md	8.92	$(7/2^-)$	$(7/2^-)$	0	0.12	0.802	1.355×10^{-21}	0.1198	0.0845	−0.80	0.27
^{255}Rf→^{251}No	9.06	$(9/2^-)$	$(7/2^+)$	1	0.62	0.866	1.382×10^{-21}	0.0344	0.0675	−0.84	0.33
^{259}Rf→^{255}No	9.13	$3/2^+$#	$(1/2^+)$	2	0.49	0.800	1.949×10^{-21}	0.0357	0.0528	−0.96	0.32
^{261}Rf→^{257}No	8.65	$3/2^+$#	$(3/2^+)$	0	1.06	0.861	1.134×10^{-22}	0.1531	0.0733	0.25	1.38
^{257}Db→^{253}Lr	9.21	$9/2^+$#	$(7/2^-)$	1	0.26	0.861	1.780×10^{-21}	0.0616	0.0642	−0.95	0.24
^{263}Db→^{259}Lr	8.84	$9/2^+$#	$1/2^-$#	5	1.80	0.832	1.690×10^{-23}	0.1935	0.0351	1.09	2.54
^{259}Sg→^{255}Rf	9.77	$(11/2^-)$	$(9/2^-)$	2	−0.48	0.847	2.378×10^{-20}	0.0257	0.0506	−2.07	−0.77
^{261}Sg→^{257}Rf	9.71	$(3/2^+)$	$(1/2^+)$	2	−0.72	0.874	1.791×10^{-20}	0.0576	0.0484	−1.96	−0.64

Continued on next page

Table 2-continued from previous page

α transition	Q_α	j_p^π	j_d^π	$\ell_{\min}$	$\log_{10}T_{1/2}^{\exp}$	F	P	$P_\alpha^{\exp}$	P_α^{Eq}	$\log_{10}T_{1/2}^{\mathrm{cal1}}$	$\log_{10}T_{1/2}^{\mathrm{cal2}}$
^{263}Sg→^{259}Rf	9.41	$3/2^+$#	$3/2^+$#	0	0.03	0.802	4.560×10^{-21}	0.0438	0.0651	−1.33	−0.14
^{265}Sg→^{261}Rf	9.05	$11/2^-$#	$3/2^+$#	5	1.26	0.863	3.526×10^{-23}	0.3101	0.0330	0.75	2.23
^{261}Bh→^{257}Db	10.51	$(5/2^-)$	$9/2^+$#	3	−1.89	0.836	5.991×10^{-19}	0.0266	0.0393	−3.46	−2.06
^{265}Hs→^{261}Sg	10.47	$3/2^+$#	$(3/2^+)$	0	−2.72	0.817	6.846×10^{-19}	0.1611	0.0561	−3.51	−2.26
^{269}Hs→^{265}Sg	9.28	$9/2^+$#	$11/2^-$#	1	1.18	0.841	3.727×10^{-22}	0.0362	0.0502	−0.26	1.04
^{267}Ds→^{263}Hs	11.78	$3/2^+$#	$3/2^+$#	0	−5.00	0.810	1.664×10^{-16}	0.1274	0.0478	−5.89	−4.57

Table 3. Same as Tables 1 and 2 but for 28 odd-odd nuclei.

α transition	Q_α	j_p^π	j_d^π	$\ell_{\min}$	$\log_{10}T_{1/2}^{\exp}$	F	P	$P_\alpha^{\exp}$	P_α^{Eq}	$\log_{10}T_{1/2}^{\mathrm{cal1}}$	$\log_{10}T_{1/2}^{\mathrm{cal2}}$
^{224}Pa→^{220}Ac	7.69	(5^-)	(3^-)	2	−0.07	0.868	1.488×10^{-21}	0.1559	0.0417	-0.88	0.50
^{226}Pa→^{222}Ac	6.99	1^-#	1^-	0	2.16	0.873	7.997×10^{-24}	0.1698	0.0608	1.39	2.61
^{228}Pa→^{224}Ac	6.27	3^+	(0^-)	3	6.63	0.764	2.338×10^{-27}	0.0225	0.0437	4.98	6.34
^{230}Pa→^{226}Ac	5.44	2^-	(1^-)	2	10.67	0.791	2.180×10^{-31}	0.0212	0.0581	9.00	10.23
^{224}Np→^{220}Pa	9.33	2^-#	1^-#	2	−4.42	0.842	1.617×10^{-17}	0.3308	0.0344	-4.90	-3.44
^{226}Np→^{222}Pa	8.34	()	1^-#	0	−1.46	0.884	5.278×10^{-20}	0.1059	0.0508	-2.43	-1.14
^{228}Np→^{224}Pa	7.54	4^+#	(5^-)	1	2.18	0.841	1.105×10^{-22}	0.0122	0.0460	0.27	1.60
^{230}Np→^{226}Pa	6.78	4^+#	1^-#	3	3.96	0.861	5.339×10^{-26}	0.4087	0.0392	3.57	4.98
^{236}Np→^{232}Pa	5.01	(6^-)	2^-	4	15.48	0.890	1.206×10^{-35}	0.0053	0.0468	13.20	14.53
^{234}Am→^{230}Np	6.80	0^-#	4^+#	5	5.55	0.874	1.808×10^{-27}	0.3058	0.0288	5.04	6.58
^{236}Am→^{232}Np	6.26	5^-	5^-	0	6.73	0.856	1.041×10^{-28}	0.3582	0.0610	6.28	7.50
^{234}Bk→^{230}Am	8.11	3^-#	1^-	2	2.24	0.871	2.003×10^{-22}	0.0057	0.0346	-0.01	1.45
^{240}Es→^{236}Bk	8.27	4^-#	4^+	1	0.93	0.857	1.993×10^{-22}	0.1179	0.0343	1.64	1.47
^{242}Es→^{238}Bk	8.16	2^+#	1#	1	1.49	0.849	9.438×10^{-23}	0.0692	0.0330	0.33	1.81
^{244}Es→^{240}Bk	7.95	6^+#	7^-	1	2.96	0.840	1.964×10^{-23}	0.0114	0.0324	1.02	2.51
^{246}Es→^{242}BK	7.65	4^-#	3^+	1	3.66	0.815	1.766×10^{-24}	0.0261	0.0324	2.08	3.57
^{248}Es→^{244}Bk	7.16	2^-#	4^-#	2	5.76	0.869	1.599×10^{-26}	0.0215	0.0298	4.09	5.62
^{252}Es→^{248}Bk	6.74	(4^+)	6^+	2	7.72	0.842	2.896×10^{-28}	0.0134	0.0293	5.85	7.38
^{244}Md→^{240}Es	8.95	3^+#	4^-#	1	−0.42	0.863	5.377×10^{-21}	0.0972	0.0290	-1.43	0.11
^{246}Md→^{242}Es	8.90	1^-#	2^+#	1	−0.04	0.849	4.204×10^{-21}	0.0527	0.0277	-1.32	0.24
^{250}Md→^{246}Es	8.16	2^-#	4^-#	2	2.87	0.821	1.482×10^{-23}	0.0190	0.0247	1.15	2.76
^{256}Md→^{252}Es	7.75	(1^-)	(4^+)	3	4.70	0.870	3.956×10^{-25}	0.0099	0.0199	2.70	4.40
^{258}Md→^{254}Es	7.27	8^-#	7^+	1	6.65	0.858	1.338×10^{-26}	0.0033	0.0268	4.17	5.75
^{252}Lr→^{248}Md	9.17	7^-#	()	0	−0.08	0.775	7.252×10^{-21}	0.0367	0.0284	-1.52	0.03
^{254}Lr→^{250}Md	8.83	4^+#	2^-#	3	1.40	0.816	2.711×10^{-22}	0.0309	0.0184	-0.11	1.63
^{256}Lr→^{252}Md	8.86	$(0^-,3^-)$#	1^+	1	1.52	0.843	8.642×10^{-22}	0.0071	0.0224	-0.63	1.02
^{256}Db→^{252}Lr	9.34	9^-#	7^-#	2	0.36	0.862	2.931×10^{-21}	0.0297	0.0193	-1.17	0.55
^{258}Db→^{254}Lr	9.44	0^-#	4^+#	1	0.75	0.845	8.770×10^{-21}	0.0041	0.0205	-1.64	0.05

are relatively small when the nucleons occupy the closed shell or magic number. This pattern implies that the shell effect has a key role in α-particle preformation [59]. In addition, the apparent odd-even staggering effect in Fig. 1 can be considered a valid object to further investigate the strong interaction. A similar odd-even effect also occurs in the one-neutron and one-proton separation energies [60]. Kaneko *et al.* found that α-particle condensation is enhanced by the strong proton-neutron interaction [61]. Therefore, α-particle preformation is restricted by mul-

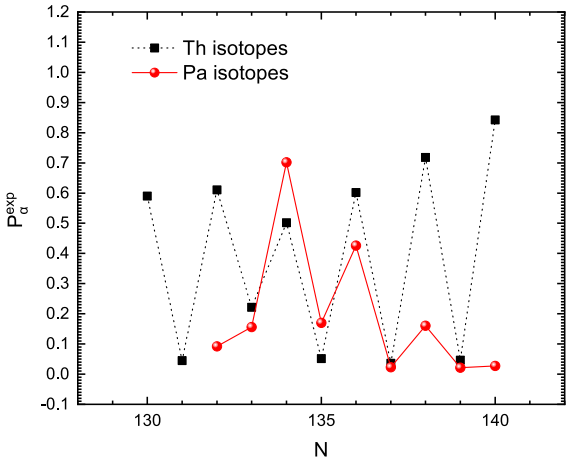

Fig. 1. (color online) Experimental α-particle preformation factor P_α^{exp} extracted from Eq. (14). The black squares and red balls denote the corresponding results of Th and Pa isotopes, respectively.

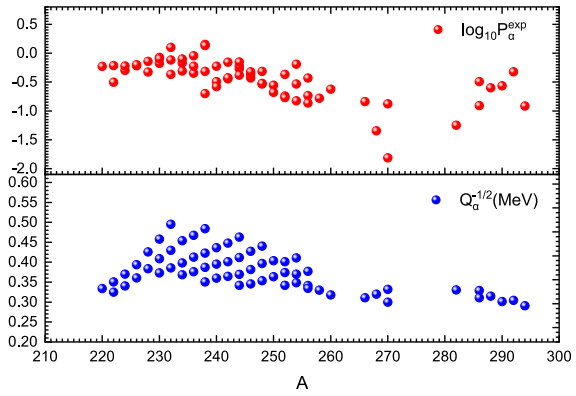

Fig. 2. (color online) Variations in the logarithmic values of extracted experimental α-particle formation factors $\log_{10}P_\alpha^{Exp}$ (red) and the reciprocal of the square root of α decay energy $Q_\alpha^{-1/2}$ (blue) against mass numbers for even-even nuclei.

tiple factors.

Combined with the above discussion, for those nuclei with exact experimental data, the corresponding preformation factors can be extracted using Eq. (14). However, no effective method exists for evaluating the α-particle preformation factors of unknown nuclei under the TPA framework. Whether the preformation factor can be reasonably evaluated has aroused our interest. In this contribution, we aim to construct a simple analytical expression to estimate preformation factors; thus, the corresponding physical factors associated with the α-particle preformation factors are of interest.

An important feature to be considered is the relationship between the preforamtion factors and decay energy. As we know, the Q_α value determines the penetration probability and further affects the decay process. Deng *et al*. revealed a close agreement between the logarithmic values of extracted experimental α-particle preformation factors $\log_{10}P_\alpha^{exp}$ and the reciprocal of the square root of α decay energy $Q_\alpha^{-1/2}$ [62]. For a more intuitive presentation, the corresponding results for even-even nuclei are plotted as a function of mass numbers A in Fig. 2. This figure shows that the variation trend of $\log_{10}P_\alpha^{exp}$ and $Q_\alpha^{-1/2}$ is consistent. This result indicates that the α decay energy can be considered a well-described quantity for estimating α-particle preformation factors. Additinally, we must consider the nuclear structure information. In a study on proton radioactivity [63, 64], Delion *et al*. revealed an apparent linear decline relationship between proton preformation factors and $A^{1/3}$(A is the mass number of the parent nuclei). They suggested that this performance is derived from the asymptotic exponential behavior of the proton wave function on the nuclear surface. It is worthwhile to explore whether a similar linear relationship exists in the α decay process because these two decay modes share the same decay mechanism. For further investigation, we plot the logarithmic values of extracted experimental α-particle preformation factors $\log_{10}P_\alpha^{exp}$ versus $A^{1/3}$ in Fig. 3. The figure shows that the preformation factors decrease gradually with the increase in mass number, and the fitting line satisfies the corresponding variation trend. This result means that $A^{1/3}$ can also be considered a valid physical quantity to describe α-particle preformation factors from another perspective.

In summary, we primarily observe that two physical quantities $Q_\alpha^{-1/2}$ and $A^{1/3}$ exhibit considerable regularity in the estimation of α-particle preformation factors. The discussion suggests that the unpaired nucleons inhibit α-particle preformation. Additionally, some studies have shown that for unfavored α decay, the corresponding centrifugal potential generated by the nonzero angular momentum inhibit the formation of α-particles on the surface of the parent nuclei [62]. Based on these analyses and capturing the main physical factors, we further propose a simple analytical expression to estimate α-particle preformation factors:

$$\log_{10}P_\alpha^{Eq} = aZQ_\alpha^{-1/2} + bA^{1/3} + c + d\sqrt{l(l+1)} + h, \qquad (15)$$

where Z and A are the proton and mass numbers of the parent nucleus, respectively. The first term is dependent on the α decay energy. The second and third terms jointly describe the relationship between preformation factors and $A^{1/3}$. The fourth term represents the contribution of the centrifugal potential to α-particle preformation. The last term denotes the blocking effect derived from the unpaired nucleons. The h value of even-even nuclei is equal to 0 because the parent nuclei have no unpaired nucleons. For odd-A and odd-odd nuclei, the value of blocking effect h of odd-odd nuclei is twice the corresponding value of odd-A nuclei owing to presence of unpaired nucleons.

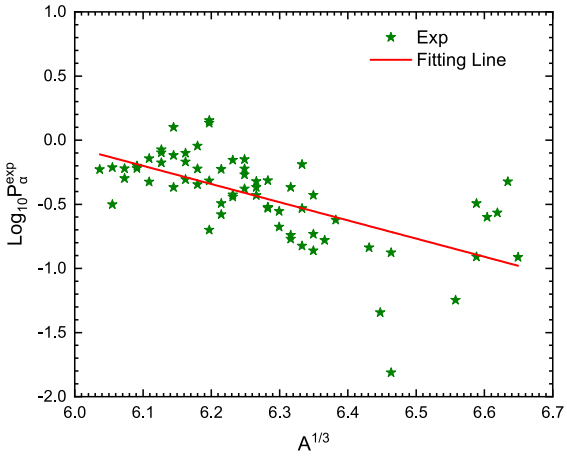

Fig. 3. (color online) Logarithm of the experimental α-particle formation factors versus $A^{1/3}$ for even-even nuclei.

By fitting the extract experimental α-particle preformation factors, we list the values of adjustable parameters in Table 4. The table shows that the values of b, d, and h are all negative. The negative value of b indicates that the preformation factors should decline as the mass number A increases. This result is consistent with the linear decline relationship shown in Fig. 3. The negative values of d and h also suggest that both the centrifugal potential and unpaired nucleons inhibit α-particle preformation. Using this formula, we systematically calculate the α-particle preformation factors denoted as $P_{\alpha}^{\rm Eq}$ and listed in Tables 1−3 for even-even, odd-A, and odd-odd nuclei, respectively.

Generally, the standard deviation can reflect the agreement between the experimental α-particle preformation factors extracted using Eq. (14) and those estimated using Eq. (15). In this work, it is defined as follows

$$\sigma = \sqrt{\sum(\log_{10}P_{\alpha}^{\rm Eq} - \log_{10}P_{\alpha}^{\rm exp})^2/n}, \tag{16}$$

where $\log_{10}P_{\alpha}^{\rm Eq}$ and $\log_{10}P_{\alpha}^{\rm exp}$ are the logarithmic forms of estimated and experimental α-particle preformation factors, respectively, and n is the number of nuclei involved for each case. The corresponding standard deviations for 65 even-even, 87 odd-A, 28 odd-odd, and all nuclei calculated using Eq. (16) are listed in Table 4. The table shows that Eq. (15) with only five valid parameters can effectively reproduce the extracted experimental α-particle preformation factors. For a more intuitive comparison, the experimental α-particle preformation factors derived from Eq. (14) and estimated using Eq. (15) for even-even, odd-A, and odd-odd nuclei are plotted in Figs. 4−6, respectively. These figures show that the estimated α-particle preformation factors are relatively close to the experimental ones for even-even nuclei. However, the results for odd-A and odd-odd nuclei are not very satisfactory. For a clear description, we form two separate regions in Figs. 5 and 6 and interestingly find that the estimated and experimental α-particle factors are in good agreement in the light yellow region with neutron number $N > 141$. The large discrepancy from the other region as shown in Figs. 5 and 6 prompts us to provide a reasonable explanation. Tracing back to each stage, after a detailed analysis, we believe that the corresponding difference is largely owing to the uneven nuclear data affecting the balance of parameter values, *i.e.*, h of the blocking effect. Considering the overall performance, the corresponding deviations may be understandable and acceptable.

Table 4. Parameters of Eq. (15) and standard deviations between α-particle preformation factors estimated using Eq. (15) and those extracted using Eq. (14).

Number	Nuclei	a	b	c	d	h	σ
65	Even-Even nuclei						0.244
87	Odd-A nuclei	0.035	−1.406	7.070	−0.054	−0.4687	0.601
28	Odd-Odd nuclei					−0.9374	0.575
180	All nuclei						0.468

In the following, we list the calculated α decay half-lives with $P_0 = 1$ denoted as $\log_{10}T_{1/2}^{\rm cal1}$ in Tables 1−3 for even-even, odd-A, and odd-odd nuclei, respectively. Moreover, the α-particle preformation factors estimated using Eq. (15) are used to calculate α decay half-lives, which are denoted as $\log_{10}T_{1/2}^{\rm cal2}$ and listed in the same tables. For a clear comparison, the deviations between experimental α decay half-lives and the two calculated ones in the logarithmic form for even-even, odd-A, and odd-odd nuclei are plotted in Figs. 7−9, respectively. The figures show large deviations between $\log_{10}T_{1/2}^{\rm cal1}$ and the experimental α decay half-lives. After the estimated α-particle preformation factors are considered, $\log_{10}T_{1/2}^{\rm cal2}$ can reproduce the experimental data well, as shown by green shaded regions in Figs. 7−9. The excellent performances suggest that this analytical expression can not only effectively evaluate the α-particle preformation factors but also facilitate the accurate calculation of half-lives.

As an application, this analytical expression is used to estimate the α-particle preformation factors and further predict corresponding half-lives for unknown even-even nuclei with $Z = 118$ and 120. The Q_{α} value is extremely important for predicting α decay half-lives, and the estimation of corresponding preformation factors is also related to decay energy, as shown in Eq. (15). For more scientific predictions, two credible mass models, FRDM [65] and WS4+ [66], are used to predict α decay energy. The detailed results are listed in Table 5. In this table, the first three columns denote α transition, experimental α decay energy, and half-lives, respectively. The fourth and fifth columns represent the predicted α decay energy de-

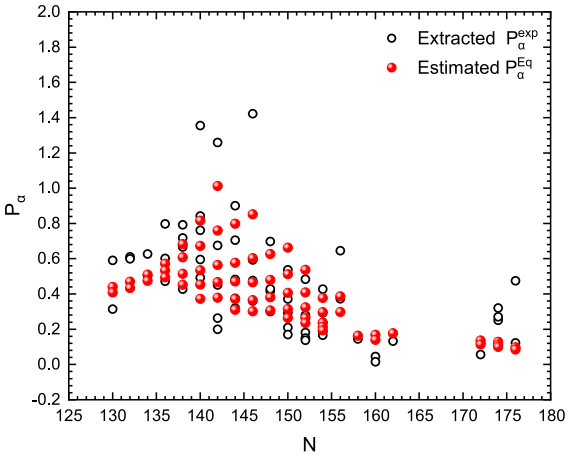

Fig. 4. (color online) Experimental α-particle preformation $P_\alpha^{\rm exp}$ extracted from Eq. (14) and the estimated ones $P_\alpha^{\rm Eq}$ using Eq. (15) for even-even nuclei. The black circles and red balls denote $P_\alpha^{\rm Exp}$ and $P_\alpha^{\rm Eq}$, respectively.

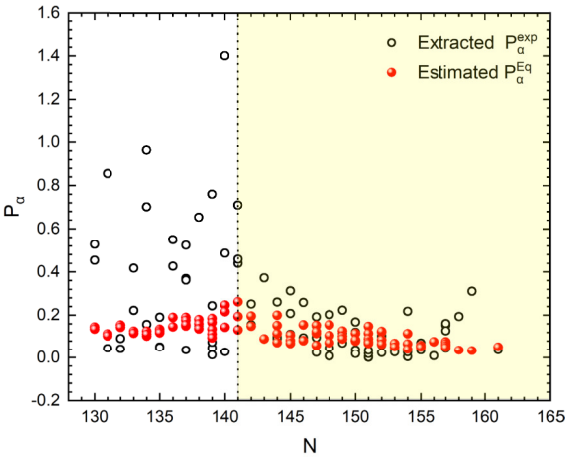

Fig. 5. (color online) Same as Fig. 4 but for odd-A nuclei.

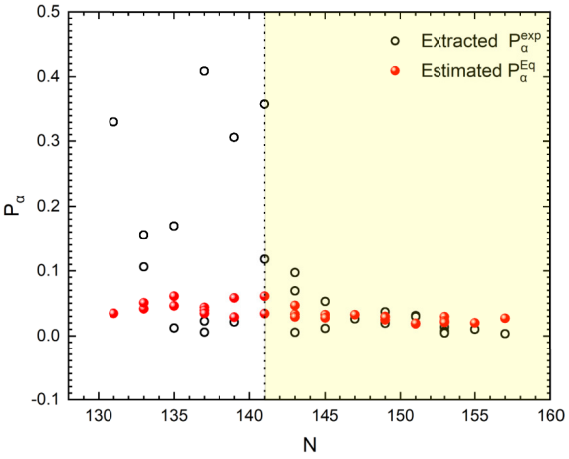

Fig. 6. (color online) Same as Figs. 4 and 5 but for odd-odd nuclei.

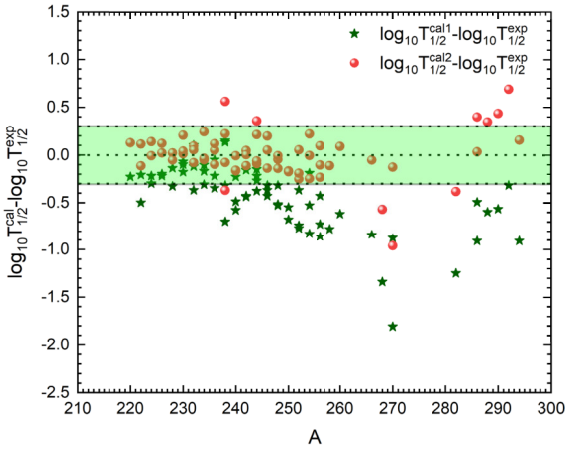

Fig. 7. (color online) Differences in logarithmic form between experimental α decay half-lives and two calculated ones for even-even nuclei. The green stars and red balls denote the differences caused by $\log_{10}T_{1/2}^{\rm cal1}$ and $\log_{10}T_{1/2}^{\rm cal2}$, respectively.

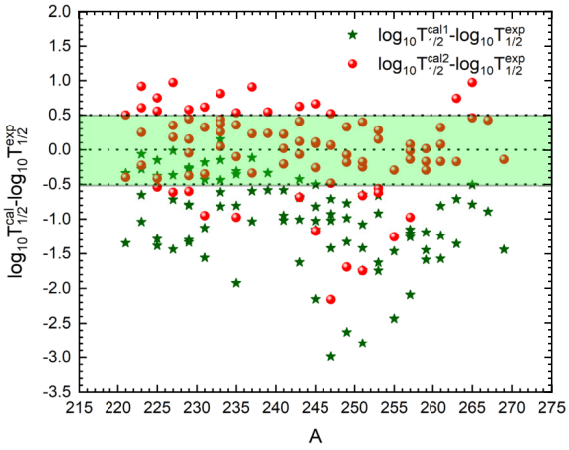

Fig. 8. (color online) Same as Fig. 7 but for odd-A nuclei.

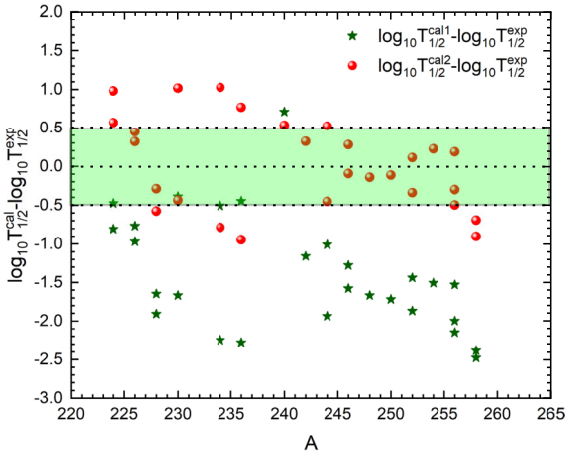

Fig. 9. (color online) Same as Figs. 7 and 8, but for odd-odd nuclei.

Table 5. α-particle preformation factors predicted using Eq. (15) and half-lives for unknown even-even nuclei with Z = 118 and 120. The predicted α decay energies are derived from the FRDM [65] and WS4+ [66] mass models. The experimental α decay energy and half-lives are obtained from the latest evaluated atomic mass table AME2020 [50, 52, 53].

α transition	$Q_\alpha^{\rm exp}$	$\log_{10}T_{1/2}^{\rm exp}$	$Q_\alpha^{\rm FRDM}$	$Q_\alpha^{\rm WS4+}$	$P_\alpha^{\rm FRDM}$	$P_\alpha^{\rm WS4+}$	$\log_{10}T_{1/2}^{\rm FRDM}$	$\log_{10}T_{1/2}^{\rm WS4+}$
Nuclei with Z=118								
^{288}Og→^{284}Lv	–	–	12.88	12.59	0.0883	0.0991	−5.05	−4.48
^{290}Og→^{286}Lv	–	–	12.81	12.57	0.0847	0.0868	−4.93	−4.46
^{292}Og→^{288}Lv	–	–	12.37	12.21	0.0845	0.0860	−4.07	−3.74
^{294}Og→^{290}Lv	11.87	−3.15	12.28	12.17	0.0813	0.0823	−3.89	−3.67
^{296}Og→^{292}Lv	–	–	12.29	11.73	0.0773	0.0825	−3.89	−2.71
^{298}Og→^{294}Lv	–	–	12.51	12.16	0.0719	0.0748	−4.39	−3.63
^{300}Og→^{296}Lv	–	–	12.72	11.93	0.0670	0.0731	−4.83	−3.21
Nuclei with Z=120								
^{296}120→^{292}Og	–	–	13.69	13.32	0.0700	0.0726	−6.05	−5.34
^{298}120→^{294}Og	–	–	13.36	12.98	0.0689	0.0716	−5.46	−4.70
^{300}120→^{296}Og	–	–	13.40	13.29	0.0654	0.0661	−5.56	−5.36
^{302}120→^{298}Og	–	–	13.72	12.87	0.0604	0.0658	−6.15	−4.57
^{304}120→^{300}Og	–	–	13.83	12.74	0.0569	0.0636	−6.33	−4.33
^{306}120→^{302}Og	–	–	14.27	13.76	0.0521	0.0546	−7.11	−6.26
^{308}120→^{304}Og	–	–	14.31	12.94	0.0495	0.0566	−7.20	−4.76

rived from the FRDM and WS4+ mass models, respectively. The sixth and seventh columns represent the preformation factors predicted using Eq. (15) based on corresponding decay energy. The last two columns represent the predicted α decay half-lives in terms of Q_α from the FRDM and WS4+ mass models, denoted as $\log_{10}T_{1/2}^{FRDM}$ and $\log_{10}T_{1/2}^{WS4+}$, respectively. The table shows that decay energy is essential in the prediction of the related half-lives. When the differences of the decay energy are within a small range, the predicted results of the related half-lives are almost consistent. The uncertainty of 1 MeV in the decay energy can lead to the uncertainty of the related half-lives with a factor of 10 or 10^2. These corresponding predictions can provide valuable references for synthesizing superheavy nuclei and/or new elements.

IV. SUMMARY

Using the Two-Potential Approach, we systematically analyze the α-particle preformation factors of heavy and superheavy nuclei from ^{220}Th to ^{294}Og. We find that the α-particle preformation factors exhibit considerable regularity, *i.e.*, an odd-even staggering effect, and unpaired nucleons inhibit α-particle preformation. In addition, the preformation factor is strongly dependent on multiple physical factors. Both decay energy and mass number of parent nucleus exhibit the certain connection with the extracted experimental α-particle preformation factors. Based on this, a simple analytical expression is proposed to estimate α-particle preformation factors. The excellent performances suggest that this analytical expression can not only evaluate the α-particle preformation factors well but also accurately calculate half-lives. With this formula, we estimate the α-particle preformation factors and further predict the corresponding α decay half-lives for unknown even-even nuclei with Z = 118 and 120. These predictions provide valuable references to further experiments in synthesizing superheavy nuclei.

Acknowledgements

We would like to thank Yang-Yang Xu, Xiao-Yan Zhu, and Prof. Yan-Zhao Wang for useful discussions.

References

[1] Z. Ren and G. Xu, Phys. Rev. C **36**, 456 (1987)
[2] X. J. Bao, S. Q. Guo, H. F. Zhang *et al.*, Phys. Rev. C **95**, 034323 (2017)
[3] C. Xu and Z. Ren, Phys. Rev. C **75**, 044301 (2007)
[4] W. M. Seif, M. Shalaby, and M. F. Alrakshy, Phys. Rev. C **84**, 064608 (2011)
[5] Y. Z. Wang, S. J. Wang, Z. Y. Hou *et al.*, Phys. Rev. C **92**, 064301 (2015)

[6] H. F. Zhang, G. Royer, Y. J. Wang *et al.*, Phys. Rev. C **80**, 057301 (2009)
[7] A. Parkhomenko and A. Sobiczewski, Acta Phys Pol. B **36**, 1363 (2005)
[8] D. S. Delion, R. J. Liotta, and R. Wyss, Phys. Rev. C **92**, 051301 (2015)
[9] Y. T. Oganessian, F. S. Abdullin, P. D. Bailey, D. E. Benker *et al.*, Phys. Rev. Lett. **104**, 142502 (2010)
[10] E. Rutherfold and H. Geiger, Proc. R. Soc. London A **81**, 162 (1908)
[11] G. Gamow, Z. Phys. **51**, 204 (1928)
[12] R. W. Gurney and E. U. Condon, Nature **122**, 439 (1928)
[13] S. Luo, X. Pan, X. H. Li *et al.*, Common. Theor. Phys. **75**, 025301 (2023)
[14] J. M. Dong, W. Zuo, J. Z. Gu *et al.*, Phys. Rev. C **81**, 064309 (2010)
[15] J. M. Dong, H. F. Zhang, Y. Z. Wang *et al.*, Eur. Phys. J. A **41**, 197 (2009)
[16] D. M. Zhang, L. J. Qi, D. X. Zhu *et al.*, Nucl. Sci. Tech. **34**, 55 (2023)
[17] D. S. Delion, S. Peltonen, and J. Suhonen, Phys. Rev. C **73**, 014305 (2006)
[18] S. B. Duarte, O. Rodriguez *et al.*, Phys. Rev. C **57**, 2516 (1998)
[19] S. Luo, Y. Y. Xu, D. X. Zhu *et al.*, Eur. Phys. J. A **58**, 244 (2022)
[20] H. M. Liu, Y. T. Zou, X. Pan *et al.*, Chin. Phys. C **44**, 094106 (2020)
[21] M. Concalves and S. B. Duarte, Phys. Rev. C **48**, 2409 (1993)
[22] P. Mohr, Phys. Rev. C **73**, 031301 (2006)
[23] Y. J. Wang, H. F. Zhang, W. Zuo *et al.*, Chin. Phys. Lett. **27**, 062103 (2010)
[24] J. P. Cui, Y. H. Gao, Y. Z. Wang *et al.*, Nucl. Phys. A **1017**, 122341 (2022)
[25] F. Z. Xing, H. Qi, G. C. Yong *et al.*, Nucl. Phys. A **1028**, 122528 (2022)
[26] K. Varga, R. G. Lovas, and R. J. Liotta, Phys. Rev. Lett. **69**, 37 (1992)
[27] I. Tonozuka and A. Arima, Nucl. Phys. A **323**, 45 (1979)
[28] G. Dodig-Crnković, F. Janouch, and R. Liotta *et al.*, Nucl. Phys. A **444**, 419 (1985)
[29] G. Röpke, P. Schuck, Y. Funaki *et al.*, Phys. Rev. C **90**, 034304 (2014)
[30] C. Xu, Z. Ren, G. Röpke *et al.*, Phys. Rev. C **93**, 011306 (2016)
[31] S. M. S. Ahmed, R. Yahaya, and S.Radiman, Rom. Rep. Phys. **65**, 1281 (2013)
[32] S. M. S. Ahmed, Nucl. Phys. A **962**, 103 (2017)
[33] D. M. Deng and Z. Ren, Phys. Rev. C **93**, 044326 (2016)
[34] C. Xu and Z. Ren, Nucl. Phys. A **760**, 303 (2005)
[35] G. Royer, J. Phys. G: Nucl. Part. Phys. **26**, 1149 (2000)
[36] H. F. Zhang, W. Zuo, J. Q. Li *et al.*, Phys. Rev. C **74**, 017304 (2006)
[37] X. J. Bao, H. F. Zhang, B. S. Hu *et al.*, J. Phys. G: Nucl. Part. Phys. **39**, 095103 (2012)
[38] J. Bocki, J. Randrup, W. wiatecki *et al.*, Ann. Phys. (N. Y.) **105**, 427 (1977)
[39] X. D. Sun, P. Guo, and X. H. Li, Phys. Rev. C **93**, 034316 (2016)
[40] Y. B. Qian and Z. Z. Ren, Phys. Rev. C **85**, 027306 (2012)
[41] Y. B. Qian and Z. Z. Ren, Nucl. Phys. A **852**, 82 (2011)
[42] C. Xu and Z. Ren, Nucl. Phys. A **778**, 1 (2006)
[43] V. Yu. Denisov and A. A. Khudenko, Phys. Rev. C **80**, 034603 (2009)
[44] S. A. Gurvitz and G. Kalbermann, Phys. Rev. Lett. **59**, 262 (1987)
[45] J. J. Morehead, J. Math. Phys. **36**, 5431 (1995)
[46] V. Yu. Denisov and A. A. Khudenko, Atom. Data Nucl. Data Tabl. **95**, 815 (2009)
[47] X. D. Sun, P. Guo, and X. H. Li, Phys. Rev. C **94**, 024338 (2016)
[48] J. G. Deng, J. C. Zhao, D. Xiang *et al.*, Phys. Rev. C **45**, 024318 (2017)
[49] J. L. Chen, X. H. Li, X. J. Wu *et al.*, Eur. Phys. J. A **57**, 305 (2021)
[50] F. G. Kondev, M. Wang, W. J. Huang *et al.*, Chin. Phys. C **45**, 030001 (2021)
[51] https://www.nndc.bnl.gov
[52] W. J. Huang, M. Wang, F. G. Kondev *et al.*, Chin. Phys. C **45**, 030002 (2021)
[53] M. Wang, W. J. Huang, F. G. Kondev *et al.*, Chin. Phys. C **45**, 030003 (2021)
[54] Y. Z. Wang, J. Z. Gu, and Z. Y. Hou, Phys. Rev. C **89**, 047301 (2014)
[55] H. F. Zhang and G. Royer, Phys. Rev. C **77**, 054318 (2008)
[56] B. Buck, A. C. Merchant, and S. M. Perez, Phys. Rev. C **45**, 2247 (1992)
[57] C. Xu and Z. Ren, Phys. Rev. C **74**, 014304 (2006)
[58] Y. Qian, Z. Ren and D. Ni, Phys. Rev. C **83**, 044317 (2011)
[59] J. G. Deng and H. F. Zhang, Phys. Rev. C **102**, 044314 (2020)
[60] T. K. Dong and Z. Ren, Phys. Rev. C **72**, 064331 (2005)
[61] K. Kaneko and M. Hasegawa, Phys. Rev. C **67**, 041306 (R) (2003)
[62] J. G. Deng and H. F. Zhang, Phys. Lett. B **816**, 136247 (2021)
[63] D. S. Delion and A. Dumitrescu, Phys. Rev. C **103**, 054325 (2021)
[64] C. Qi, D. S. Delion, R. Wyss *et al.*, Phys. Rev. C **85**, 011303 (R) (2012)
[65] Möller P, Nix J R, and Swiatecki W J, At. Data and Nucl. Data Tables **59**, 185 (1995)
[66] N. Wang, M. Liu, X. Z. Wu *et al.*, Phys. Lett. B **734**, 215 (2014)